J|A|C|S COMMUNICATIONS

Published on Web 03/04/2010

Solution-Phase Synthesis of SnSe Nanocrystals for Use in Solar Cells

Matthew A. Franzman, Cody W. Schlenker, Mark E. Thompson, and Richard L. Brutchey*

Department of Chemistry and the Center for Energy Nanoscience and Technology, University of Southern California, Los Angeles, California 90089

Received January 11, 2010; E-mail: brutchey@usc.edu

The need for cost-effective, efficient, and environmentally friendly photovoltaic materials continues to fuel new research in the field of semiconductor nanocrystal synthesis.[1] The I−III−VI family of semiconductor nanocrystals, such as $CuInS_2$, $CuInSe_2$, and $CuIn_xGa_{1-x}Se_2$, has shown significant promise as an environmentally friendly alternative to cadmium- and lead-based photovoltaic materials.[2] For example, solar cells derived from nanocrystal inks of $CuIn_xGa_{1-x}S_2$ were recently shown to demonstrate power conversion efficiencies of up to 5.55%.[2c] However, the ever-increasing demand for copper and the increasing costs and limited supplies of indium and gallium place the long-term feasibility of these materials as solar cell components into question.[3] Thus, there is a need to develop new types of semiconductor nanocrystals that are composed of more earth-abundant elements.

Recently, tin(II) selenide (SnSe) has garnered interest as an earth-abundant and environmentally benign component of photovoltaic devices such as solar cells.[4] Bulk SnSe has an indirect band gap of 0.90 eV and a direct band gap of 1.30 eV,[5] while thin films of SnSe have demonstrated band gaps that are higher in energy as a result of quantum confinement.[4a] While significant advances in the synthesis of related IV−VI semiconductor nanocrystals (e.g., SnS and SnTe) have been made,[6] there has been comparatively less success in the synthesis of well-defined SnSe nanocrystals. To date, there have been no reports of phase-pure SnSe nanocrystals synthesized by a solution-phase route that are small enough to exhibit quantum confinement. This communication presents the first solution-phase synthesis of well-defined and quantum-confined SnSe nanocrystals and demonstrates their utility in solar cells.

Dialkyl dichalcogenides have proven to be useful precursors for the solution-phase synthesis of a variety of semiconductor nanocrystals at relatively low temperatures.[7] As such, SnSe nanocrystals were synthesized using a related procedure wherein di-*tert*-butyl diselenide (0.38 mmol) was injected into a solution of anhydrous tin(II) chloride (0.74 mmol) in a mixture of dodecylamine and dodecanethiol (2.50 and 0.50 mL, respectively) at 95 °C. After the reaction solution was heated to 180 °C for 4 min and then cooled, the SnSe nanocrystals were precipitated using ethanol to yield a dark-brown solid that was dispersible in common organic solvents such as toluene. Adding a stoichiometric amount (i.e., 1 molar equiv of selenium relative to tin) of di-*tert*-butyl diselenide yielded phase-pure SnSe (see below). Addition of excess diselenide (i.e., 2 molar equiv of selenium relative to tin) yielded crystalline berndtite $SnSe_2$ (JCPDS no. 01-089-3197). Thus, by controlling the amount of di-*tert*-butyl diselenide in the reaction, the composition of the nanocrystals (and the oxidation state of tin) can be rationally controlled.

Transmission electron microscopy (TEM) revealed elongated, anisotropic nanocrystals 19.0 ± 5.1 nm wide but more polydisperse in length (Figure 1). The high-resolution TEM image in Figure 1a shows an apparent single-crystalline particle with the (111) lattice planes displayed (d = 0.29 nm). Previous solution-phase syntheses

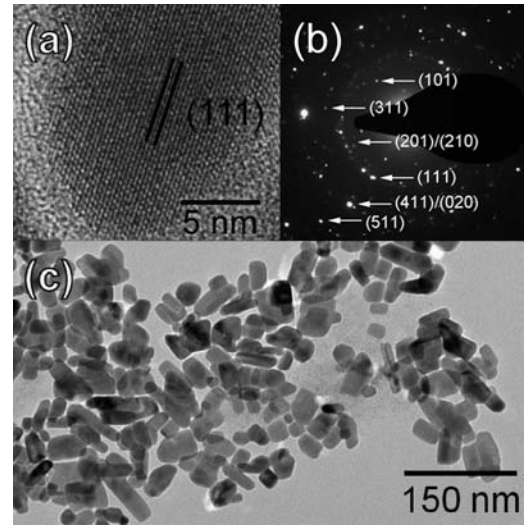

Figure 1. TEM images of SnSe nanocrystals. (a) High-resolution TEM image of a single nanocrystal. (b) SAED pattern indexed to SnSe. (c) Low-resolution TEM image of SnSe nanocrystals.

of SnSe resulted in larger nano- and microscale products with rod and sheet morphologies.[8] Powder X-ray diffraction (XRD) analysis of the SnSe nanocrystals revealed that they crystallized in the orthorhombic phase (*Pnma*), which consists of a series of strongly bound double layers of tin and selenium in a highly distorted rock salt structure.[4a] The lattice parameters a = 11.55 Å, b = 4.16 Å, and c = 4.45 Å calculated from the diffraction pattern are in good agreement with literature values for orthorhombic SnSe (JCPDS no. 048-1224). Moreover, the XRD pattern suggests that the SnSe nanocrystals are phase-pure, without any evidence of crystalline SnO, SnO_2, $SnSe_2$, or Se byproducts (Figure S1 in the Supporting Information). The lattice parameters calculated from selected-area electron diffraction (SAED) patterns of several randomly chosen regions of the SnSe nanocrystals agreed with the lattice parameters calculated from the XRD pattern for orthorhombic SnSe (Figure 1b). The elemental composition of the nanocrystals was confirmed to be near-stoichiometric (48:52 Sn/Se) by energy-dispersive X-ray spectroscopy (EDX) (Figure S2). X-ray photoelectron spectroscopy (XPS) was used to corroborate the elemental composition (49:51 Sn/Se) and confirm the oxidation states of tin and selenium in the nanocrystals. The Sn $3d_{5/2}$ peak at 485.6 eV and Se $3d_{5/2}$ peak at 53.6 eV are consistent with the binding energies for Sn^{2+} and Se^{2-} previously reported for SnSe (Figure S3).[8a]

The SnSe nanocrystals absorb through the entire visible spectrum into the near-IR (Figure S4), resulting in the dark-brown color of the material. The direct optical band gap of the SnSe nanocrystals (E_g = 1.71 eV) is blue-shifted relative to the direct band gap for bulk SnSe (E_g = 1.30 eV). Nanocrystalline thin films of SnSe with a grain size of ∼15 nm were previously synthesized by chemical

10.1021/ja100249m

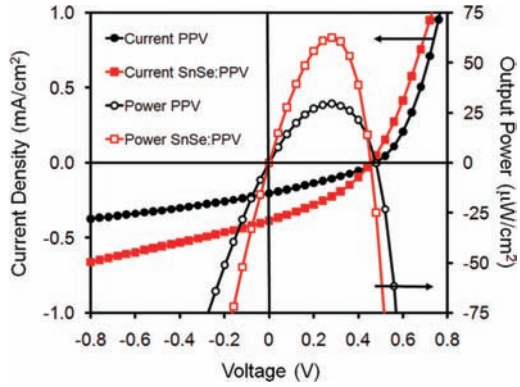

Figure 2. Overlaid spectral-mismatch-corrected $J(V)$ (solid symbols) and $P(V)$ (open symbols) characteristics for ITO/MoO_3/poly/PTCDI/LiF/Al devices, where poly is a 0.25:1.0 (w/w) SnSe:PPV film (red curves) or a neat PPV polymer film (black curves) under 1000 W m^{-2} AM 1.5G illumination.

bath deposition.[4b] The direct band gap of these thin films (E_g = 1.74 eV) is also greater than the bulk band gap. Thus, nanocrystals in the size regime reported here are small enough to exhibit apparent quantum confinement effects.

To assess the potential of these SnSe nanocrystals to act as electron-accepting materials in photovoltaics, we compared hybrid solar cells to neat polymer devices. The hybrid devices consisted of a 100 Å MoO_3 hole-transport layer, a 350 Å SnSe:poly[2-methoxy-5-(3′,7′-dimethyloctyloxy)-1,4-phenylenevinylene] (PPV) absorbing layer (0.25:1.0 w/w), a 200 Å perylene-3,4,9,10-tetracarboxylic diimide (PTCDI) acceptor/hole-blocking layer, and a LiF (10 Å)/Al (1000 Å) bilayer cathode on glass/ITO substrates. The spectral-mismatch-corrected current densities as functions of voltage, $J(V)$, measured under one-sun illumination for the SnSe:PPV hybrid films and neat PPV films are overlaid in Figure 2, as are the output power densities as functions of voltage, $P(V)$. The short-circuit current density (J_{SC}) of the SnSe:PPV hybrid device (0.39 mA cm^{-2}) was nearly twice that of the neat polymer control (0.20 mA cm^{-2}), while the open-circuit voltage (V_{OC}) of the former (455 mV) was comparable to that of the latter (480 mV). The fill factors for the SnSe:PPV hybrid (0.36) and PPV-based (0.30) devices were similar, suggesting no charge trapping on SnSe. Moreover, the power conversion efficiency (η_P) was enhanced by 100% (η_P = 0.06% for SnSe:PPV, compared with η_P = 0.03% for neat PPV). This enhancement resulted from doubling of the quantum efficiency near 500 nm, which was attributed to electron transfer from PPV to SnSe since the hybrid film absorption coefficient is comparable to that of neat PPV at 500 nm (Figure S5). Substituting C_{60}/2,9-dimethyl-4,7-diphenyl-1,10-phenanthroline (BCP) for PTCDI/LiF gave η_P > 0.25% for SnSe:PPV; however, the reliability of these devices was compromised by rapid degradation (Figure S6), which has been previously reported for PPV/C_{60} organic photovoltaics.[9]

In summary, a facile solution-phase synthesis of well-defined SnSe nanocrystals that exhibit quantum confinement effects has been reported for the first time. The direct optical band gap E_g = 1.71 eV matches reasonably well with the solar spectrum, making these nanocrystals attractive candidates for incorporation into solar cells. Functional solar cells were fabricated using a SnSe:PPV active layer combined with PTCDI or C_{60}/BCP acceptor layers under AM 1.5G illumination. Future studies will focus on the optimization of these low-cost devices to best utilize this earth-abundant photovoltaic material.

Acknowledgment. This material is based on work supported by the National Science Foundation under DMR-0906745. M.A.F. was supported as part of the Center for Energy Nanoscience, an Energy Frontier Research Center funded by the U.S. Department of Energy, Office of Science, Office of Basic Energy Sciences, under Award DE-SC0001013. C.W.S. was supported by the Center for Advanced Molecular Photovoltaics (CAMP) (KUS-C1-015-21), made by King Abdullah University of Science and Technology (KAUST) and Global Photonic Energy Corporation.

Supporting Information Available: Experimental details; XRD, EDX, XPS, and UV−vis−NIR results; absorption coefficient and quantum efficiency of films; device data; and AFM images. This material is available free of charge via the Internet at http://pubs.acs.org.

References

(1) (a) Sargent, E. H. *Nat. Photonics* **2009**, *3*, 325. (b) Hillhouse, H. W.; Beard, M. C. *Curr. Opin. Colloid Interface Sci.* **2009**, *14*, 245. (c) Kamat, P. V. *J. Phys. Chem. C* **2008**, *112*, 18737.
(2) (a) Pan, D.; Wang, X.; Hong Zhou, Z.; Chen, W.; Xu, C.; Lu, Y. *Chem. Mater.* **2009**, *21*, 2489. (b) Xie, R.; Rutherford, M.; Peng, X. *J. Am. Chem. Soc.* **2009**, *131*, 5691. (c) Guo, Q.; Ford, G. M.; Hillhouse, H. W.; Agrawal, R. *Nano Lett.* **2009**, *9*, 3060. (d) Tang, J.; Hinds, S.; Kelley, S. O.; Sargent, E. H. *Chem. Mater.* **2008**, *20*, 6906. (e) Panthani, M. G.; Akhavan, V.; Goodfellow, B.; Schmidtke, J. P.; Dunn, L.; Dodabalapur, A.; Barbara, P. F.; Korgel, B. A. *J. Am. Chem. Soc.* **2008**, *130*, 16770.
(3) (a) Wadia, C.; Alivisatos, A. P.; Kammen, D. M. *Environ. Sci. Technol.* **2009**, *43*, 2072. (b) Ragnarsdottir, K. V. *Nat. Geosci.* **2008**, *1*, 720. (c) Gordon, R. B.; Bertram, M.; Graedel, T. E. *Proc. Natl. Acad. Sci. U.S.A.* **2006**, *103*, 1209.
(4) (a) Pejova, B.; Tanusevski, A. *J. Phys. Chem. C* **2008**, *112*, 3525. (b) Pejova, B.; Grozdanov, I. *Thin Solid Films* **2007**, *515*, 5203.
(5) Lefebvre, I.; Szymanski, M. A.; Olivier-Fourcade, J.; Jumas, J. C. *Phys. Rev. B* **1998**, *58*, 1896.
(6) (a) Xu, Y.; Al-Salim, N.; Bumby, C. W.; Tilley, R. D. *J. Am. Chem. Soc.* **2009**, *131*, 15990. (b) Hickey, S. G.; Waurisch, C.; Rellinghaus, B.; Eychmuller, A. *J. Am. Chem. Soc.* **2008**, *130*, 14978. (c) Kovalenko, M. V.; Heiss, W.; Shevchenko, E. V.; Lee, J.-S.; Schwinghammer, H.; Alivisatos, A. P.; Talapin, D. V. *J. Am. Chem. Soc.* **2007**, *129*, 11354.
(7) (a) Norako, M. E.; Brutchey, R. L. *Chem. Mater.* **2010**, *22*, 1613. (b) Webber, D. H.; Brutchey, R. L. *Chem. Commun.* **2009**, 5701. (c) Norako, M. E.; Franzman, M. A.; Brutchey, R. L. *Chem. Mater.* **2009**, *21*, 4299. (d) Franzman, M. A.; Brutchey, R. L. *Chem. Mater.* **2009**, *21*, 1790. (e) Franzman, M. A.; Perez, V.; Brutchey, R. L. *J. Phys. Chem. C* **2009**, *113*, 630.
(8) (a) Han, Q.; Zhu, Y.; Wang, X.; Ding, W. *J. Mater. Sci.* **2004**, *39*, 4643. (b) Shen, G.; Chen, D.; Jiang, X.; Tang, K.; Liu, Y.; Qian, Y. *Chem. Lett.* **2003**, *32*, 426. (c) Schlecht, S.; Budde, M.; Kienle, L. *Inorg. Chem.* **2002**, *41*, 6001. (d) Zhang, W.; Yang, Z.; Liu, J.; Zhang, L.; Hui, Z.; Yu, W.; Qian, Y.; Chen, L.; Liu, X. *J. Cryst. Growth* **2000**, *217*, 157.
(9) (a) Jorgensen, M.; Norrman, K.; Krebs, F. C. *Sol. Energy Mater. Sol. Cells* **2008**, *92*, 686. (b) Neugebauer, H.; Brabec, C. J.; Hummelen, J. C.; Janssen, R. A. J.; Sariciftci, N. S. *Synth. Met.* **1999**, *102*, 1002.

JA100249M